doi: 10.22564/rbgf.

EFFICIENCY OF EDDY TRANSPORTS AND NONGEOSTROPHIC EFFECTS DURING THE LIFE CYCLE OF A BAROCLINIC INSTABILITY

V.B. Rao and R.F.C. Marques

Instituto Nacional de Pesquisas Espaciais - INPE
C.P. 515, 12201-970, São José dos Campos, SP, Brasil

Correlation coefficients between the meridional wind and zonal wind and temperature can be used to define the efficiency of eddy transport of momentum and heat. We used such a definition and found that medium-scale baroclinic eddies become efficient in transporting heat and momentum during the mature stage of the life cycle. The correlation coefficients between eddy momentum transports and momentum efficiency and eddy heat transports and heat efficiency are significantly high showing that efficiencies are associated with higher momentum and heat transport. We found that nongeostrophic components are more for the momentum transport than for the heat transport. We calculated the contribution of nongeostrophic components for different forms of the energies and also for the energy conversion. It is found that the highest contribution of nongeostrophic components is for eddy available potential energy which is around 40% and the lowest is for conversion term between zonal and perturbation available potential energies which is around 10%.

A EFICIÊNCIA DO TRANSPORTE TURBULENTO E OS EFEITOS NÃO-GEOSTRÓFICOS DURANTE O CICLO DE VIDA DE UMA INSTABILIDADE BAROCLÍNICA *Os coeficientes de correlação entre o vento meridional e temperatura e entre o vento meridional e zonal podem ser usados para definir a eficiência dos transportes turbulentos de calor e momentum, respectivamente. Com o uso desta definição, encontrou-se que o distúrbio baroclínico de média-escala é mais eficiente em transportar calor e momentum durante o estágio de maturidade de seu ciclo de vida. Os coeficientes de correlação entre o transporte de momentum turbulento e eficiência do transporte de momentum e o transporte de calor turbulento e a eficiência do transporte de calor são altamente significativos, mostrando que eficiências estão associadas com maior transporte de momentum e calor. Verificou-se também que os componentes não-geostróficos são maiores para o transporte de momentum do que para o transporte de calor. Calculou-se também a contribuição dos componentes não-geostróficos para energia potencial disponível zonal e turbulenta e energia cinética zonal e turbulenta e suas conversões. Encontrou-se que a maior contribuição dos componentes não-geostróficos foi para a energia potencial disponível (em torno de 40%) e a menor para o termo de conversão entre energia potencial disponível zonal e turbulenta (em torno de 10%).*

INTRODUCTION

In a series of papers Randel and Stanford (1983, 1985a, 1985b and 1985c) studied the dynamics of medium-scale waves (zonal wave numbers 4-7) in the Southern Hemisphere (S.H.) during summer. Their analysis clearly showed several charateristics of these medium-scale baroclinic waves, such as the selection of zonal scale, eastward phase propagation, baroclinic growth and barotropic decay. Randel and Stanford (1985c) examined what they called a clean example of the life cycle of baroclinic instability. They compared the observed charateristics of baroclinic instability with modelled properties of the nonlinear baroclinic waves reported by Simmons and Hoskins (1978) and found good agreement. Randel and Stanford also noted that the characteristics of baroclinic waves in the S.H. compare well with the characteristics of their counterparts in the N.H., thereby showing the basic nature of baroclinic instability in the atmosphere.

One of the fundamental properties associated with the growth and decay of baroclinic waves is the transport of heat and momentum by these waves. Then, the question that arises is: How efficient are these waves in transporting heat and momentum? In the present paper we study the efficiency of baroclinic waves in transporting heat and momentum. Our results show that during the mature stage baroclinic waves are particularly efficient in transporting heat and momentum.

In their study of medium-scale waves, Randel and Stanford (1985a, 1985c) used geostrophic approximation in calculating horizontal wind components. It would be interesting to calculate the contribution of nongeostrophic effects in wind components for the heat and momentum transports and also for the energetics. This is the second objective of the present paper.

DATA AND ANALYSIS

Our basic data are the geopotential height and wind fields provided by National Meteorological Center (NMC). Temperature is determined from geopotential height using hydrostatic approximation. As mentioned in the introduction, we propose to calculate the nongeostrophic components and these are obtained as the differences between the observed wind and geostrophic wind. Earlier Randel and Stanford (1985c) have shown the reliability of NMC data in calculating heat and momentum transports and energetics for the Southern Hemisphere during the summer.

Geopotential height and wind data are given at intervals of 2.5° longitude and 2.5° latitude and for 7 standard pressure levels between 1000hPa and 100hPa. Grid point data are subjected to harmonic analysis and heat and momentum transports, efficiencies and energetics are calculated for some individual waves and also for certain wave bands.

DEFINITION OF EFFICIENCY

Oort and Rasmusson (1971) used the degree of correlation between the meridional velocity (v) and the parameter to be transported (either zonal velocity, u or temperature, T) as a measure of efficiency. Such a definition of efficiency has been used earlier by Rao and Bonatti (1981) to study the efficiency of planetary waves in transporting heat and momentum during a major stratospheric warming. The efficiencies are given by:

$$E_1 = \frac{\overline{v'u'}}{\sqrt{\overline{v'^2}}\sqrt{\overline{u'^2}}}, \tag{1}$$

$$E_2 = \frac{\overline{v'T'}}{\sqrt{\overline{v'^2}}\sqrt{\overline{T'^2}}}, \tag{2}$$

where an over bar (-) denotes the zonal mean and a prime represents the deviation from the zonal mean. Eq.(1) and (2) measure the efficiency of the eddies in transporting momentum and heat, respectively. Oort and Rasmusson (1971) and Srivatsangam (1975) calculated the efficiency of eddy transports for the N.H.

Here we extend these earlier studies by computing the efficiencies of the eddy transports during the life cycles of baroclinic eddies in the S.H.

ENERGETICS

The computational analysis of energetics in this study is based on standard equations after Saltzman (1957) for an adiabatic and inviscid atmosphere. These are given by:

$$\frac{\delta K_E}{\delta t} = -C(K_E, K_z) - C(K_E, P_E), \qquad (3)$$

$$\frac{\delta K_z}{\delta t} = C(K_E - K_z) - C(K_z, P_z), \qquad (4)$$

$$\frac{\delta P_E}{\delta t} = C(P_z, P_E) + C(K_E, P_E), \qquad (5)$$

$$\frac{\delta P_z}{\delta t} = -C(P_z, P_E) + C(K_z, P_z), \qquad (6)$$

where K_z, P_z, K_E and P_E represent respectively zonal kinetic energy, zonal available potential energy, eddy kinetic energy and eddy available potential energy. The expressions for the conversion terms on the right hand side are well-known and are not given here. All the energy quantities are obtained as integrals in the latitude direction between 22.5° and 77.5°S and in the vertical between 850hPa and 100hPa. Latitudinal integration is weighted by the cosine of latitude to account for the sphericity of the earth. Vertical integrations are weighted by the density of each level, are simply summation over pressure. In the present study we propose to compute K_z,P_E, P_z and K_E, C (P_z, P_E) and C (K_E, K_z) for the period December 1978, January and February 1979 and also for the month of December 1979. In addition, we propose to calculate the term C (K_E, P_E) for the one month period of December 1979. This term involves the calculation of vertical p velocity ω ($\frac{dp}{dt}$). The method of calculation of ω is given in Appendix A.

RESULTS AND DISCUSSION

In this section we present and discuss the principal results. Since sensible heat transport is highest in the lower troposphere and since momentum transport is highest in the upper troposphere, we discuss E_2 for the lower troposphere and E_1 for the upper troposphere.

We shall examine now the efficiencies during the life of baroclinic waves. For this we chose the same period as that discussed by Randel and Stanford (1985c). Fig. 1 shows the efficiency E_2 for wave number 6 at 850hPa level for the period 9-17 December 1979, along with the eddy sensible heat transport $\overline{v'T'}$ (negative values indicate transport towards south pole) and the variances $\overline{v'^2}$ and $\overline{T'^2}$. Wave number 6 is selected since it dominates the Southern Hemisphere summer circulation (Randel and Stanford 1985a). It can be seen that the efficiency increases from 9 to the 11^{th}, remains high up to 13^{th} and then decreases. This shows the growing stage, the mature stage and the decay stage. During the mature stage the correlation coefficient (c.c.) becomes almost one. The rise and fall of efficiency are associated with increase and decrease of the sensible heat transport. The increase of efficiency during the growing stage occurs in conjunction with the increase of $\overline{v'^2}$ and $\overline{T'^2}$. From (2) this implies that the rate of increase of heat transport is more than the rate of increase of $\overline{v'^2}$ and $\overline{T'^2}$. As noted by Rao and Bonatti (1981), this has interesting implications for the tilt of the wave in the vertical and vertical propagations of the wave. Such a propagation of the wave in the vertical has been confirmed by Randel and Stanford (1985c).

Fig. 2 shows the efficiency E_2, $\overline{v'^2}$, $\overline{T'^2}$ at 700hPa level for wave number 6. Essentially a similar behaviour is seen at 700hPa level, although the maximum value of the correlation is somewhat low (0.8).

Fig. 3 shows the momentum transport efficiency, E, for wave number 6 at 300hPa level for the pe-

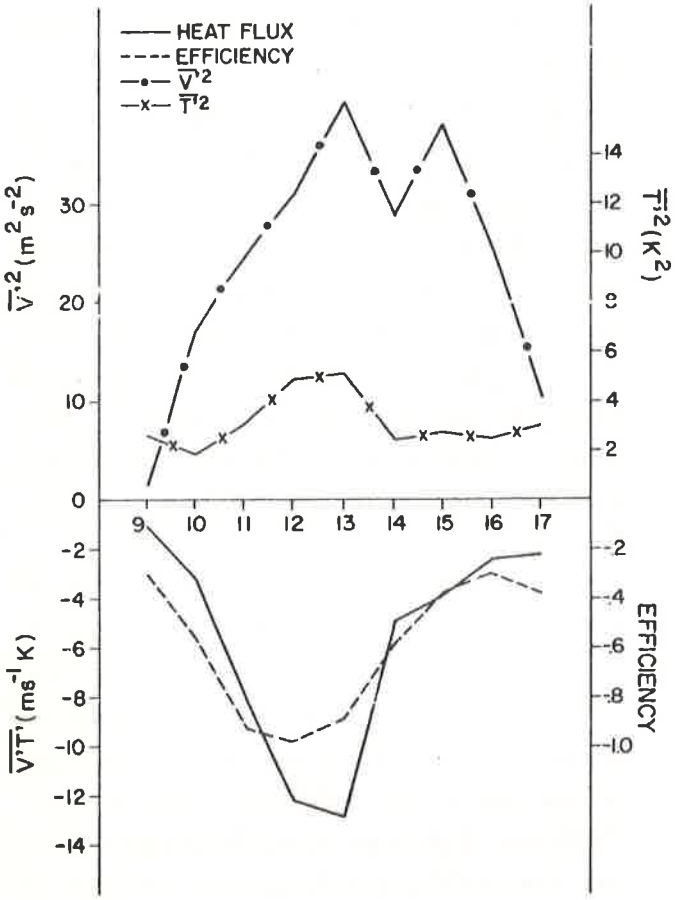

Figure 1. Efficiency of eddy transport of heat for wave number 6. Latitude 52.5°S. Level: 850hPa. Abcissa shows dates in the month of December 1979.

Eficiência do transporte de calor sensível do número de onda 6. Latitude: 52.5°. Nível: 850hPa. Abcissa mostra dados do mês de dezembro de 1979.

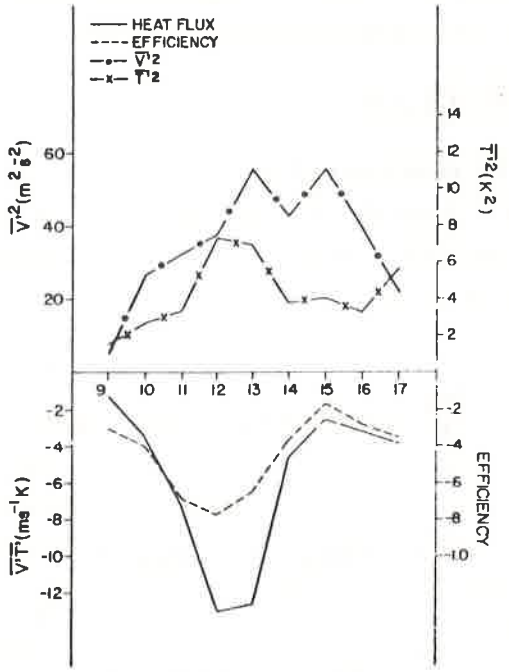

Figure 2. Same as Fig.1, but for 700hPa.

O mesmo da Fig. 1, mas para o nível de 700hPa.

riod 9-17 December 1979. For the first three days the momentum transport was towards the north and later it became southward. As shown by Randel and Stanford (1985c) this southward transport of momentum at lower latitudes was mainly responsible for the barotropic decay of medium-scale baroclinic waves. It can be seen in Fig. 3 that the efficiency of southward momentum transport increases reaching a maximum (c.c. -0.66) on 13^{th} and 14^{th} and later decreases. Thus, there is a one day lag between the maximum efficiency in heat transport and maximum efficiency in momentum transport. As in the case of heat transport increase of efficiency in Fig. 3 is associated with increase of momentum transport. The two variances $\overline{v'^2}$ and $\overline{u'^2}$ also increased from about 10^{th} reaching a maximum and then decreased. Since the sum of $\overline{v'^2}$ and $\overline{u'^2}$ can be taken as a measure of eddy kinetic energy, Fig. 3 shows the life cycle of wave number 6.

In order to find out whether similar cycles of ef-

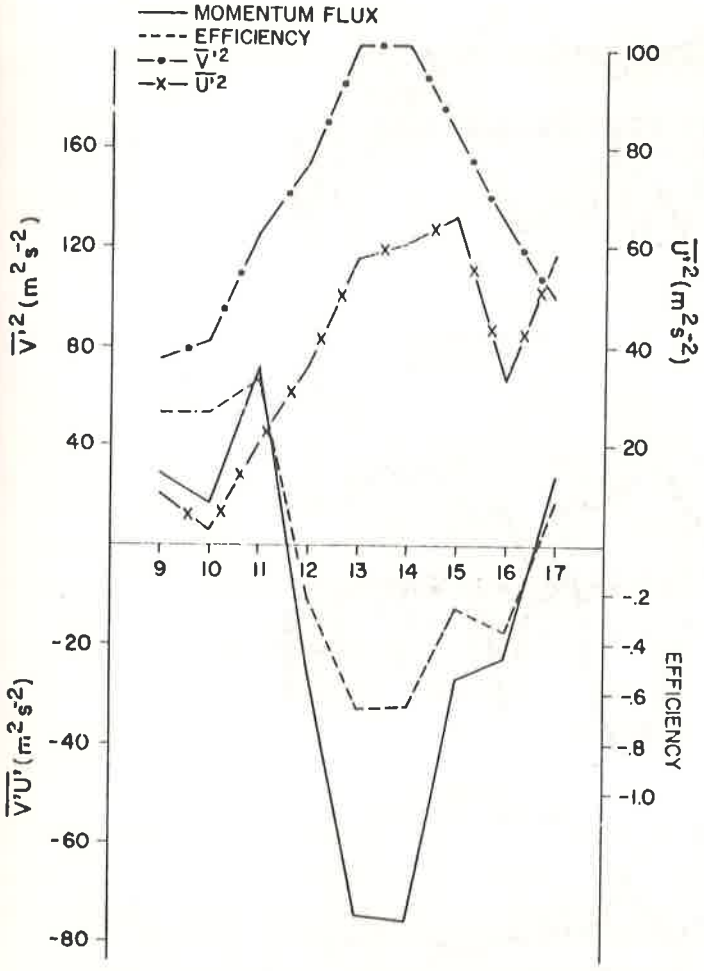

Figure 3. Efficiency of eddy transport of momentum for wave number 6. Latitude: 40°S. Level: 300hPa.

Eficiência do transporte de momentum do número de onda 6. Latitude: 40°S. Nível: 300hPa.

ficiency exist during the other periods of summer, we calculated E_1 and E_2 for the summer months of December 1978, January 1979 and February 1979. Fig. 4 shows E_2 for wave band 4-7 at 700hPa level. Also shown in the figure are the eddy heat flux and eddy kinetic energy variations. It can be seen that there are periods of high and low eddy kinetic energy indicating the life cycles of baroclinic disturbances. These cycles in eddy kinetic energy are associated with similar cycles in eddy heat transport and E_2. To find out the time lag between the eddy kinetic energy and E_1 and E_1, we calculated c.c. between eddy kinetic energy and E_1 and E_2 with different lags. The c.c. between E_2 and eddy kinetic energy shows a maximum value of -0.4 (significant as 99.5% level) with a one day lag. That is, eddy kinetic energy reaches a maximum one day after E_2 reaches highest negative values. Fig. 5 shows E_1 for wave band 4-7 at 300hPa. Eddy kinetic energy and momentum transport variations are also shown in this figure. Similar behaviour is seen in this figure, showing cycles in E_1 and eddy kinetic energy. The c.c. between E_1 and eddy kinetic energy is -0.37 (significant as 99.5% level) with a lag of two days. That is, E_1 reaches highest negative value two days after eddy kinetic energy reaches the maximum. These results show that the eddies become efficient in transporting heat one day earlier to eddy kinetic energy maximum and they become efficient in transporting momentum two days later to eddy kinetic energy maximum.

The concurrent correlation between E_1 and momentum transport is 0.89 and the concurrent correlation between E_2 and heat transport is 0.82. These high values of c.c. show the close connection between efficiencies and eddy momentum and heat transports.

ENERGETICS

Fig. 6 shows the variation of eddy kinetic energy and the conversion term C (K_E, P_E) for wave number 6 during the month of December 1979. The

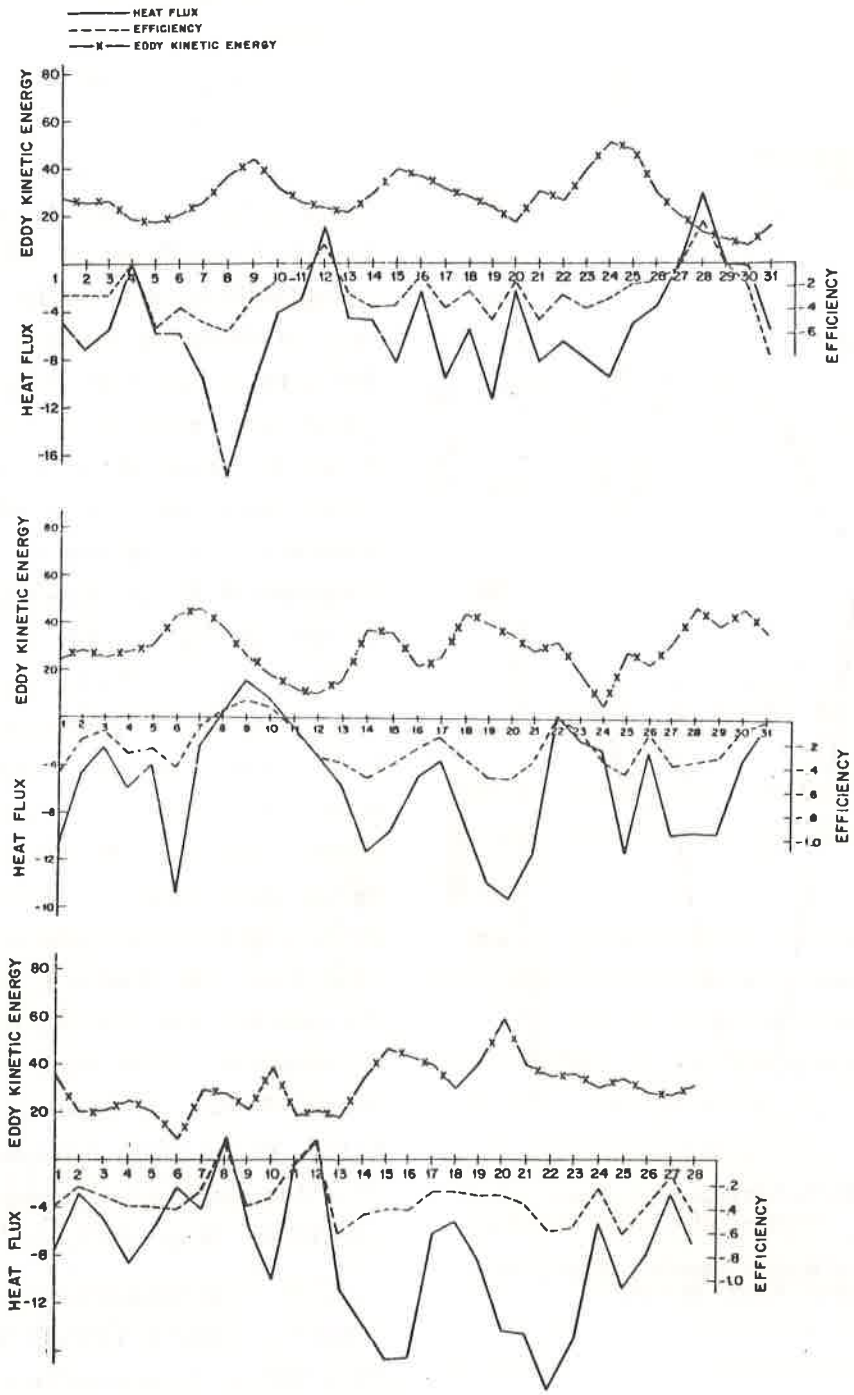

Figure 4. (a) Heat flux (m s^{-1}K). Efficiency and eddy kinetic energy (m^2 s^{-2}), for wave band 4-7 for December 1978. Latitude 45°S. Level: 700hPa. (b) Same as Fig. 4(a), but for January 1979. (c) Same as Fig. 4(a), but for February 1979.

(a) Fluxo de calor (m $s^{-1}K$). Eficiência e energia cinética turbulenta (m^2 s^{-2}), para os números de onda de 4 a 7, para dezembro de 1978. Latitude: 45°S. Nível: 700hPa. (b) Mesmo da Fig. 4(a), mas para janeiro de 1979. (c) Mesmo da Fig. 4(a), mas para fevereiro de 1979.

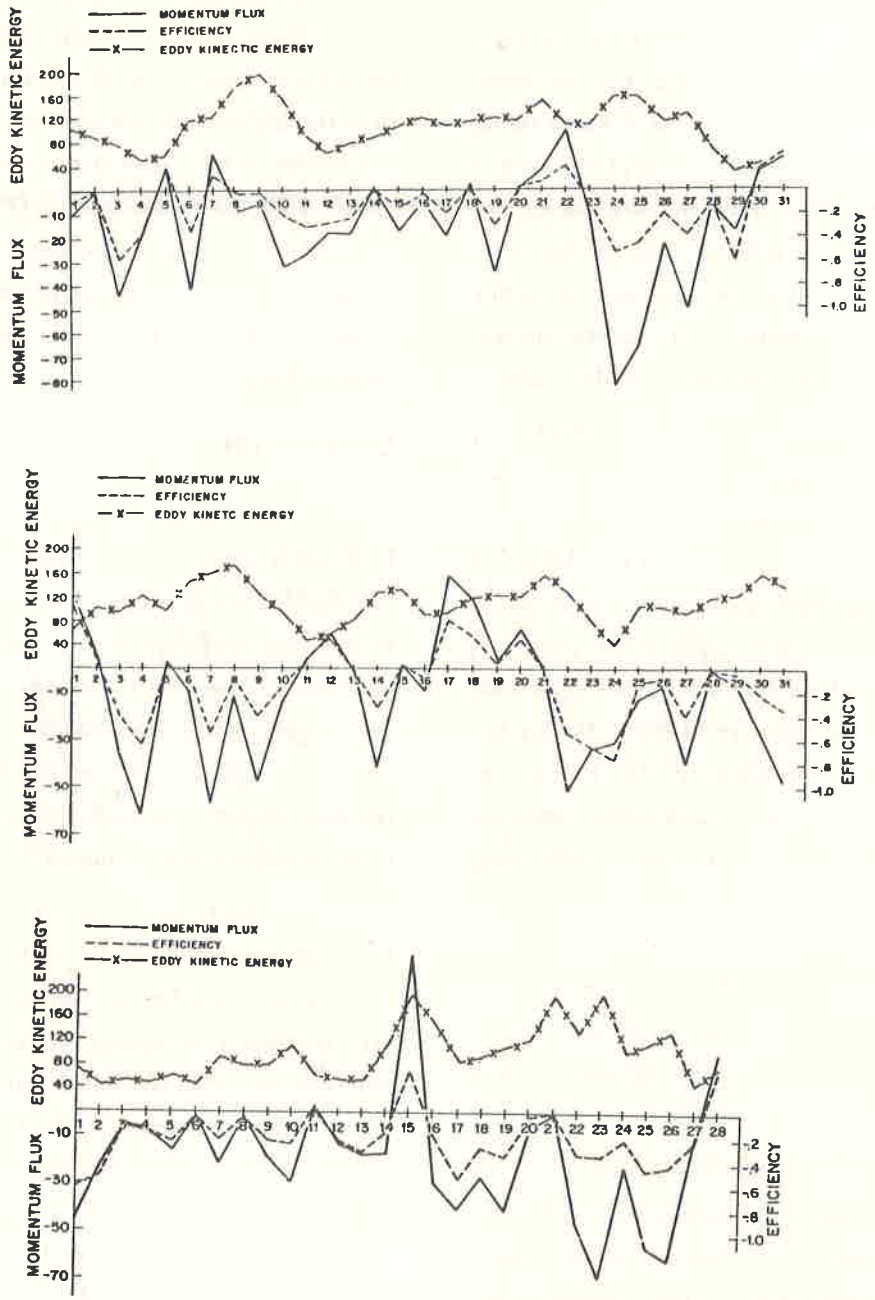

Figure 5. (a) Momentum flux ($m^2\ s^{-2}$). Efficiency and kinetic energy ($m^2\ s^{-2}$) for wave band 4-7 for December 1978. Latitude 40°S. Level: 300hPa. (b) Same as Fig. 5(a), but for January 1979. (c) Same as Fig. 5(a), but for February 1979.

(a) Fluxo de momentum ($m^2\ s^{-2}$). Eficiência e energia cinética turbulenta ($m^2\ s^{-2}$), para os números de onda de 4 a 7, para dezembro de 1978. Latitude: 40°S. Nível: 300hPa. (b) Mesmo da Fig. 5(a), mas para janeiro de 1979. (c) Mesmo da Fig. 5(a), mas para fevereiro de 1979.

high negative correlation is clearly seen, showing the importance of C (K_E, P_E) for eddy kinetic energy variations. Negative values of C (K_E, P_E) are associated with direct thermal circulation of warm rising and cold air sinking in the zonal vertical planes. Fig. 7 shows the variation of c.c. between eddy kinetic energy and C (K_E, P_E) for different lags (in days). It is seen that the c.c. reaches a maximum of about 0.7 one day prior to maximum eddy kinetic energy, remains high till one more day and then decreases.

Before starting to discuss the contribution of nongeostrophic components to the energetics, we shall briefly verify their role in the eddy transport of heat and momentum. Fig. 8 shows the difference between the observed and geostrophic transport of momentum term ($\overline{v'u'_{obs}}$ $\overline{-v'u'_{geo}}$) for the period 9-17 December 1979, which includes the life cycle case studied by Randel and Stanford (1985c). During the amplification stage of the wave (9^{th}-13^{th}), the nongeostrophic component is small and mostly negative ($\overline{v'u'_{geo}}$ ¿ $\overline{v'u'_{obs}}$). During the mature stage of the wave on 13^{th} and 14^{th}, the nongeostrophic component is large and mostly positive that is $\overline{v'u'_{geo}}$ is under estimated. On 14^{th} the nongeostrophic component in $\overline{v'u'}$ is as much as the $\overline{v'u'_{geo}}$. Thus, as the wave amplifies, the nongeostrophic effects become large reaching a maximum on 14^{th}.

Fig. 9 shows the difference between observed and geostrophic heat transport. In this case the difference is small, but the general behaviour is similar to what is seen for momentum transport. The nongeostrophic component again increases as the wave grows reaching a maximum on 13^{th} in middle latitudes. At this stage the difference $\overline{v'T'_{obs}}$ - $\overline{v'T'_{geo}}$ is about 37% of the geostrophic value.

The contribution of nongeostrophic effects for various forms of the energies and for energy conversion is calculated. Table 1 gives the mean values for 90 days (December 1978 through February 1979) for the wave band 4-7. Table 2 gives values of energies and energy conversion for wave numbers 1-10 for the same 90 days. Table 3 gives the energetics for wave number 6. In all the three tables it is seen that the highest contribution of the nongeostrophic component is for P_E, which is around 40%, and the lowest is for conversion term C (P_z, P_E). The lowest value of C (P_z, P_E) is because the nongeostrophic component in the transport of sensible heat is small as noted earlier. C (P_z, P_E) is mainly determined by sensible heat transport.

CONCLUSION

The efficiencies of meridional eddy transport of heat and momentum were calculated through the life cycles of baroclinic waves. The efficiencies of heat and momentum transport increase as the wave amplifies and they decrease as the eddies decay. The c.cs between eddy momentum transport and E_1 and eddy heat transport and E_2 are significantly high showing these higher efficiencies are associated with higher momentum and heat transport.

The conversion term C (P_E, K_E) was calculated for wave number 6 for December 1979. This term reached highest value one day before eddy kinetic energy reached a maximum and the c.c. between the two is around 0.7. We found that the nongeostrophic components were more for the momentum transport than for the heat transport. The nongeostrophic components increase as the wave grows and reach a maximum value when the eddy kinetic energy is a maximum. We calculated the contribution of nongeostrophic components for different forms of the energies and also for the energy conversions. It is found that the highest contribution of nongeostrophic components is for P, which is around 40%, and the lowest is for the conversion term C (P_z, P_E), which is around 10%.

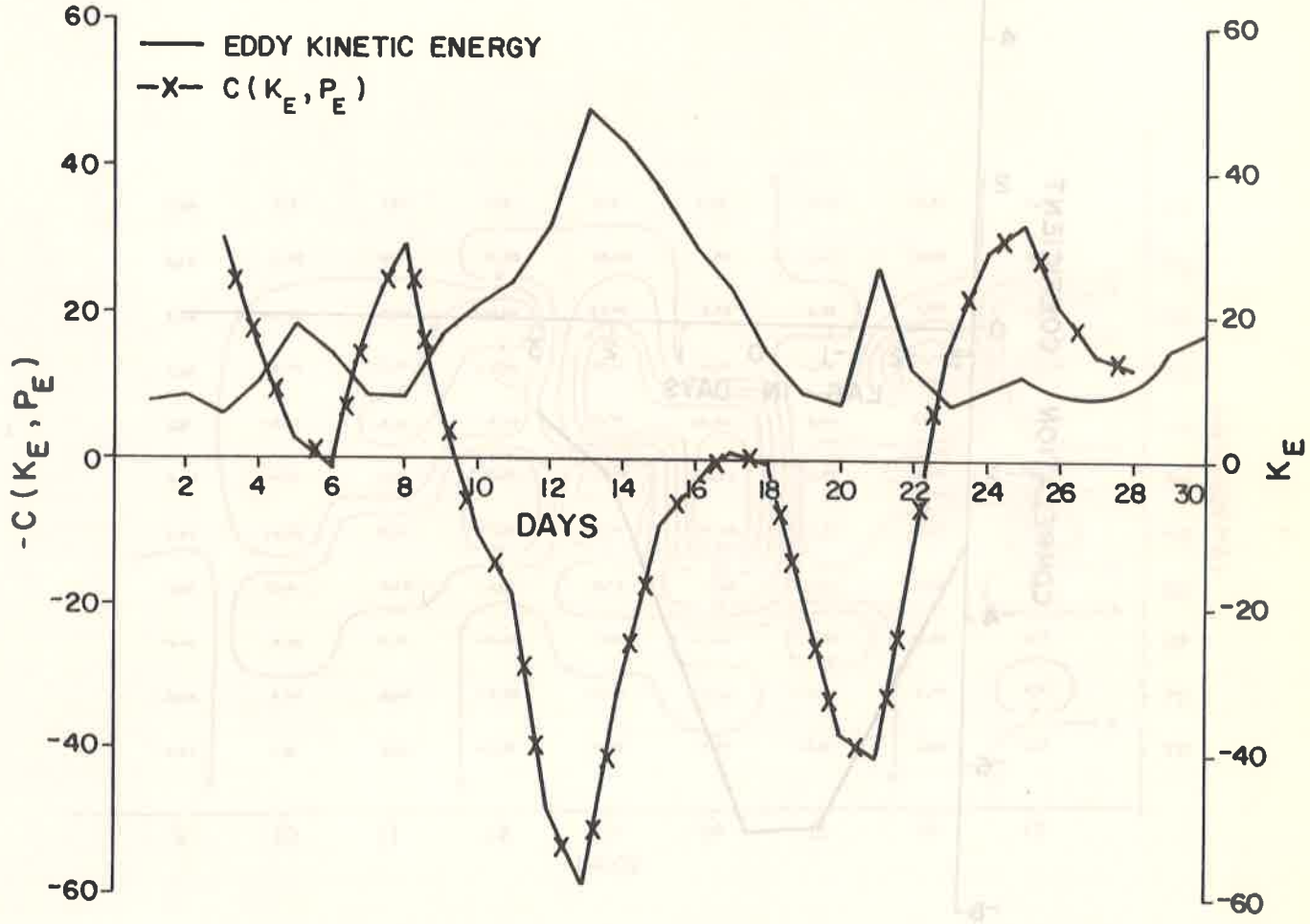

Figure 6. C (K_E, P_E) (Full line with crosses) in 10^2 J Kg day^{-1}, eddy kinetic energy in J kg^{-1} (Full line) for December 1979.

C(K_E, P_E) (linha cheia com cruz) em 10^2 J Kg dia^{-1}, energia cinética turbulenta em J kg^{-1} (Linha cheia), para dezembro de 1979.

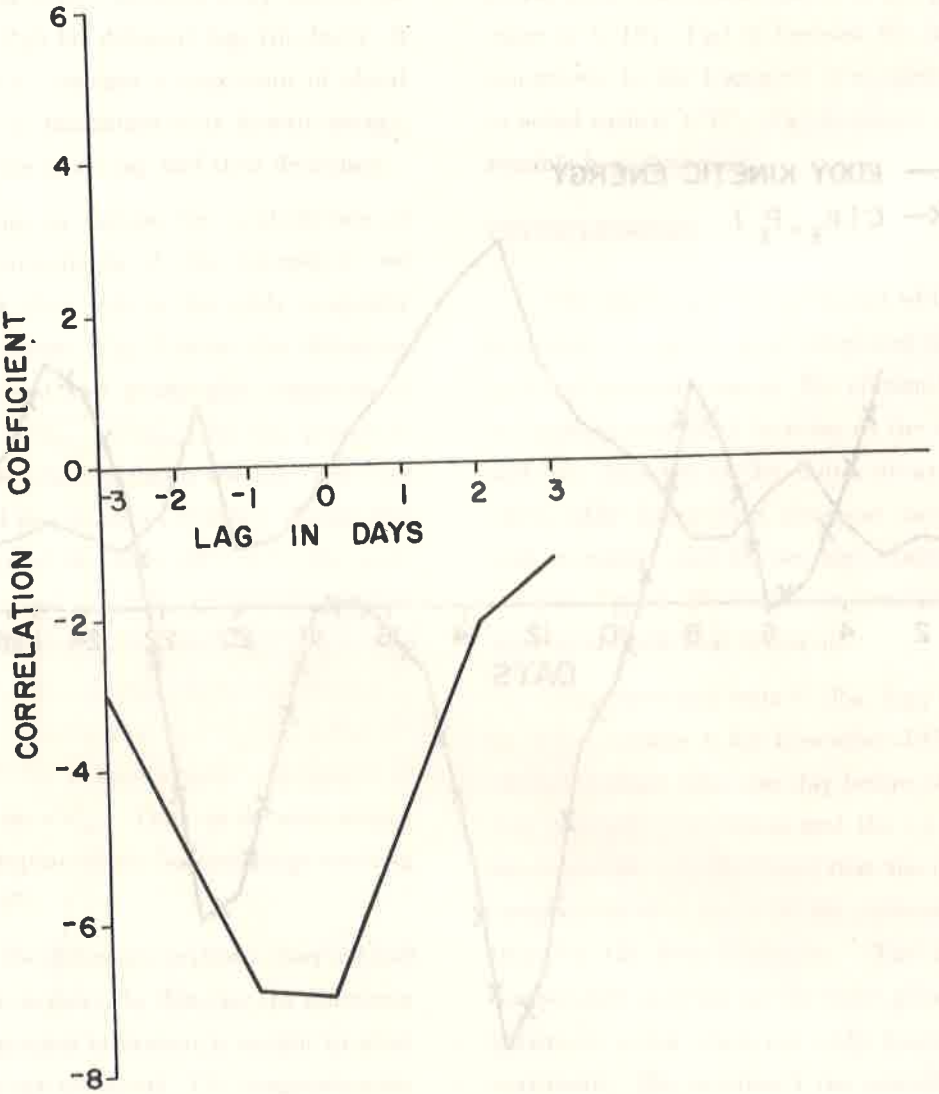

Figure 7. Correlation coefficient between the two curves of Fig. 6 for different lags.

Coeficiente de correlação entre as duas curvas da Fig. 6. Para dias simultâneos e com diferença de 1, 2 e 3 dias.

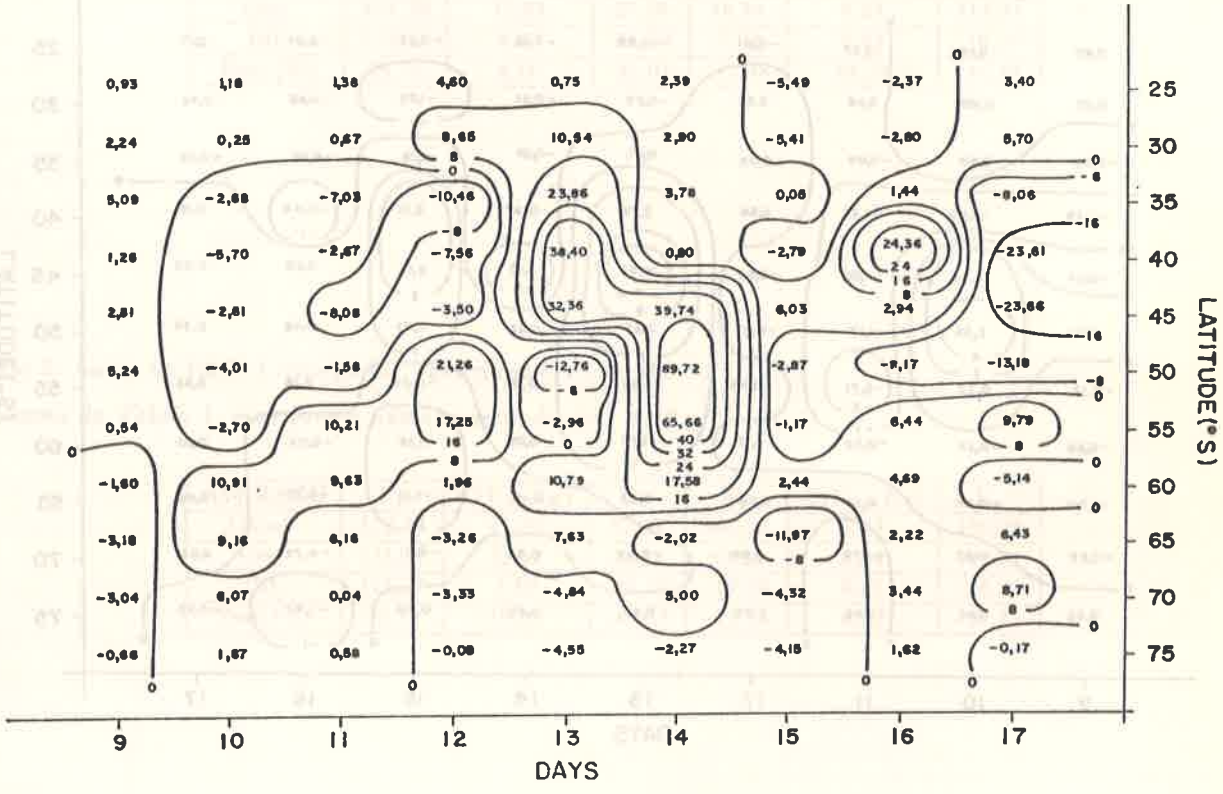

Figure 8. Isolines of difference between the momentum transport calculated with observed wind and geostrophic wind ($\overline{v'u'_{obs}}$ - $\overline{v'u'_{geo}}$). Level: 300hPa. Wave number: 6. Days in December 1979.

Isolinhas da diferença entre o transporte de momentum calculado com vento observado e geostrófico ($\overline{v'u'_{obs}}$ - $\overline{v'u'_{geo}}$). Nível: 300hPa. Número de onda 6. Dias de dezembro de 1979.

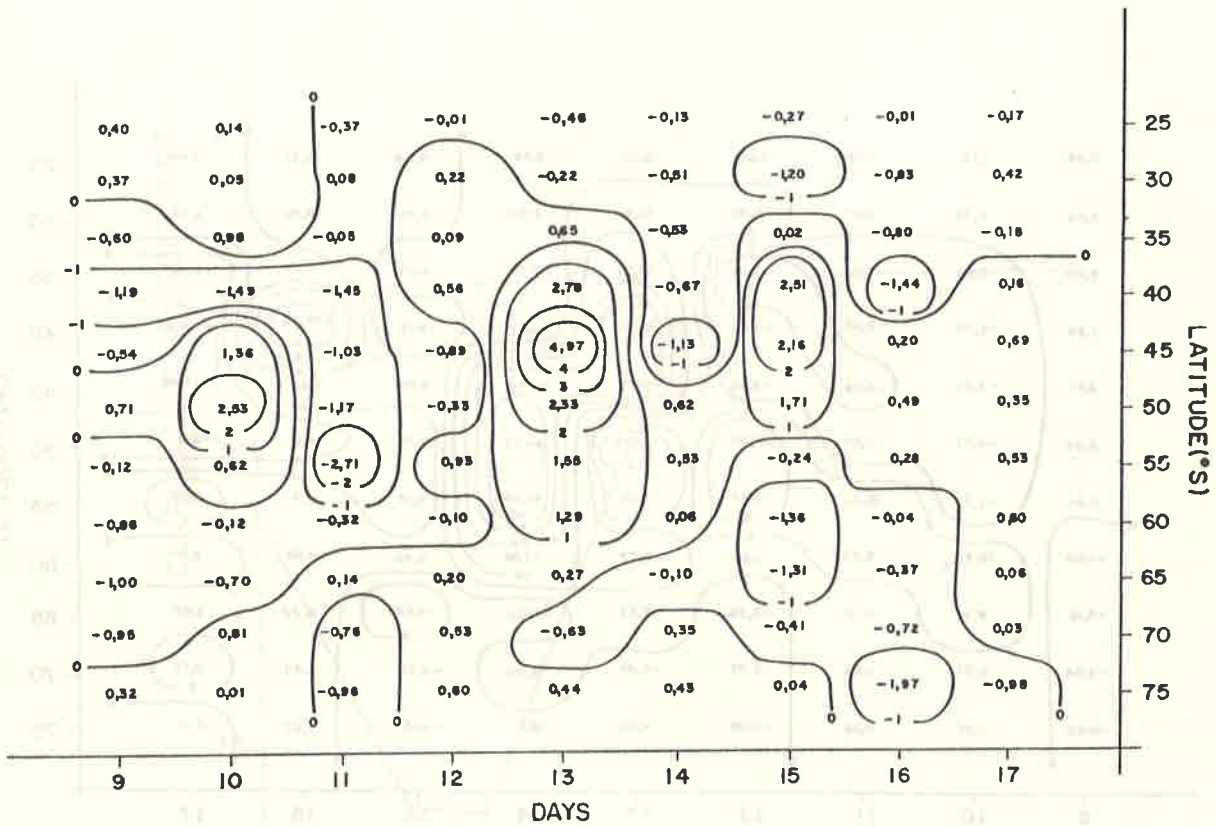

Figure 9. Isolines of difference between the heat transport. Calculated with observed wind and geostrophic wind ($\overline{v'T'_{obs}}$ - $\overline{v'T'_{geo}}$). Other details are the same as in Fig. 8.

Isolinhas da diferença entre o transporte de calor calculado com vento e temperatura observados e com vento geostrófico e temperatura hidrostática ($\overline{v'T'_{obs}}$ - $\overline{v'T'_{geo}}$). Outros detalhes são os mesmos da Fig. 8.

Table 1. 90 days (December 1978, January 1979 and February 1979) means of various energy forms and energy conversions. Wave band: 4-7: Units of P_z, P_E, K_E and K_z are 10^2 J kg^{-1}, and C(P_z, P_E) and C(K_E, K_z) are 10^2 J kg $^{-1}$ day^{-1}. Geost.: Geostrophic; Obs.: Observed; Dif.: Difference; Perc.: Percentage.

Média de 90 dias (dezembro de 1978, janeiro e fevereiro de 1979) de várias formas e conversões de energia. Número de onda de 4 a 7. Unidade de P_Z, P_E, K_Z e K_E são 10^2 J kg^{-1} e C(P_Z, P_E) e C(K_E, K_Z) são 10^2 J Kg dia^{-1}. Geost.: Geostrófico; Obs.: Observado; Dif.: Diferença e Perc.: Percentagem.

AVERAGE	P_z	C(P_z, P_E)	P_E	K_E	C(K_E, K_z)	K_z
Geost.	316,12	11,64	39,24	54,60	3,63	130,28
Obs.	431,39	12,04	27,50	46,86	4,34	113,91
Dif.	115,27	0,40	-11,74	-7,74	0,63	-16,37
Perc.(%)	26,72	4,70	-42,01	-17,38	58,25	-14,37

Table 2. Same as Table 1, except for wave numbers 1 to 10.

O mesmo da Tabela 1, mas para o número de onda de 1 a 10.

AVERAGE	P_z	C(P_z, P_E)	P_E	K_E	C(K_E, K_z)	K_z
Geost.	316,12	17,32	87,88	107,73	5,73	130,28
Obs.	431,39	19,12	62,78	89,23	6,34	113,91
Dif.	115,27	1,80	-25,11	-18,50	0,61	-16,37
Perc.(%)	26,72	10,88	-39,87	-21,23	9,62	-14,37

Table 3. Same as Table 1, except for wave numbers 6 and for 31 days (December 1979).

O mesmo da Tabela 1, mas para o número de onda 6.

AVERAGE	P_z	C(P_z, P_E)	P_E	K_E	C(K_E, K_z)	K_z
Geost.	307,86	5,09	10,44	17,33	1,64	146,12
Obs.	428,07	5,72	7,09	13,46	1,42	122,74
Dif.	120,20	0,63	-3,35	-3,87	-0,22	-23,39
Perc.(%)	28,13	38,29	-45,32	-28,75	-15,49	-19,03

APPENDIX A

Determination of ω:

Quasi-geostrophic vorticity equation is given by:

$$\frac{\delta \zeta g}{\delta t} = -V_g \cdot \nabla (\zeta_g + f) + f_o \frac{\delta \omega}{\delta p}. \qquad (1)$$

That is

$$\frac{\delta \omega}{\delta p} = \frac{1}{f_o}\left[\frac{\delta \zeta g}{\delta t} + V_g \cdot \nabla (\zeta_g + f)\right]. \qquad (2)$$

All the terms on the right hand side of A2 (R. H.S) at any level can be obtained using observed height data and using centered time differencing for the term $\frac{\delta \zeta_g}{\delta t}$. For the left hand side term $\frac{\delta \omega}{\delta p}$ centered finite differences are used. Assuming ω (1000hPa) as zero vertical velocities at other levels are determined. To ensure mass continuity the R.H.S. is averaged and the average is subtracted from each value. The present method is essentially similar to the one used earlier by Wiin-Nielsen and Brown (1960).

REFERENCES

OORT, A.H. and RASMUSSON, E.M. (1971) Atmospheric Circulation Statistics. Springfield, VA, Ntis. (NOAA, Prof. Pap. 5). 323p. Available through of Government Printing Office, Stock no 0317-0045, C55.255.

RANDEL, W. and STANFORD, J.L. (1983) Structure of Medium-scale Atmospheric Waves in Southern Hemispheric Summer. J. Atmos. Sci., 40, 2312-2318.

RANDEL, W. and STANFORD, J.L. (1985a) An Observational Study of Medium-scale Waves Dynamics in the Southern Hemispheric Summer. Part I: Waves Structure and Energetics. J. Atmos. Sci., 42, 1172-1188.

RANDEL, W. and STANFORD, J.L. (1985b) An Observational Study of Medium-scale Waves in the Southern Hemispheric Summer. Part II: Stationary-transient Wave Interface. J. Atmos. Sci., 42, 1189-1197.

RANDEL, W. and STANFORD, J.L. (1985c) The Observed Life Cycle of a Baroclinic Instability. J. Atmos. Sci., 42, 1364-1373.

RAO, V.B. and BONATTI, J.P. (1981) On the Efficiency of Meridional Eddy Transport Processes during the Major Stratospheric Warming of January 1977. Tellus, 33, 61-67.

SALTZMAN, B. (1957) Equations Governing the Energetics of the Large Scales of Atmospheric Turbulence in the Domain of Wave-number. J. Meteor., 14, 513-532.

SIMONS, A.J. and HOSKINS, B.J. (1978) The Life Cycles of Some Nonlinear Baroclinic Waves. J. Atmos. Sci., 35, 414-432.

SRIVATSANGAM, S. (1975) On the Efficiencies of Atmospheric Processes. Tellus, 27, 365-370.

WIIN-NIELSEN, A. and BROWN, J.A. (1960) On Diagnostic Computations of Atmospheric Heat Sources and Sinks and the Generation of Available Potential Energy. Proc. Int. Symp. Numer. Weather Predict. Tokyo. pp 593-613.

Submetido em 24.03.93
Revisado em 03.06.93
Aceito em 04.06.93
Editor responsável V.W.J.H. Kirchhoff

Palavras chave	Key words
Transporte turbulento	Eddy transport
Instabilidade baroclínica	Baroclinic instability
Efeitos não geostróficos	Nongeostrophic effects